



Hydrogen storage properties of LiBH₄ destabilized by SrH₂

D.M. Liu^{a,b}, W.J. Huang^a, T.Z. Si^a, Q.A. Zhang^{a,*}

^a School of Materials Science and Engineering, Anhui University of Technology, Maanshan, Anhui 243002, PR China

^b State Key Lab of Silicon Materials, Zhejiang University, Hangzhou 310027, PR China

ARTICLE INFO

Article history:

Received 20 August 2012

Received in revised form 26 September 2012

Accepted 26 September 2012

Available online 5 October 2012

Keywords:

Hydrogen storage materials

Lithium borohydride

Destabilized hydride system

Hydrogen storage properties

ABSTRACT

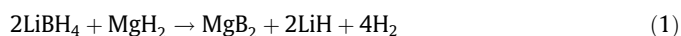
In this work, we have succeeded in destabilizing LiBH₄ by the addition of SrH₂, via the reaction $6\text{LiBH}_4 + \text{SrH}_2 \rightarrow \text{SrB}_6 + 6\text{LiH} + 10\text{H}_2$ with a theoretical hydrogen capacity of 9.1 wt.%. According to the van't Hoff and Arrhenius equations, the dehydrogenation enthalpy change and activation energy for the LiBH₄/SrH₂ system were experimentally determined to be 48 kJ/mol H₂ and 64 kJ/mol, respectively. Both are remarkably reduced in comparison with the pristine LiBH₄, which is responsible for the improved dehydrogenation property of the LiBH₄/SrH₂ system. The dehydrogenated products SrB₆ + 6LiH can be rehydrogenated to form LiBH₄ and LiSrH₃ at 723 K under an initial hydrogen pressure of 8.0 MPa.

© 2012 Elsevier B.V. All rights reserved.

1. Introduction

Hydrogen, as a highly efficient and clean secondary energy carrier, is an ideal substitute for conventional fossil fuels in the future. For large-scale utilization of hydrogen as an energy carrier, hydrogen storage systems with high efficiency and safety should be developed. Various solid-state materials, such as metal hydrides, alanes and borohydrides, have been widely investigated for this purpose. Among them, LiBH₄ is one of the most promising candidates for on-board hydrogen storage, due to its high gravimetric (18.4 wt.%) and volumetric (121 kg/m³) hydrogen density [1–3]. However, LiBH₄ alone has a reaction enthalpy change as high as 74 kJ/mol H₂ for its decomposition into LiH and B, and therefore a dehydrogenation temperature above 370 °C is required under 0.1 MPa hydrogen pressure [4]. Furthermore, the dehydrogenation process of LiBH₄ is rather sluggish and the rehydrogenation is hardly possible under mild temperature and pressure conditions [4,5].

During the last decade, LiBH₄ multicomponent reactive systems have been intensively investigated to destabilize LiBH₄ and enhance its dehydrogenation kinetics [6–20]. For example, Vajo et al. [6] reported that LiBH₄ could release hydrogen with a reduced reaction enthalpy by the addition of MgH₂, because of the change in reaction pathway as described below:



Moreover, the formation of MgB₂ could overcome the chemical inertness of pure boron, thus greatly improving the rehydrogena-

tion to form LiBH₄. Following this strategy, the LiBH₄/CaH₂ system with a small amount of catalyst was also investigated [7,21–24]. It was found that a dehydrogenation enthalpy change of 56.5 kJ/mol H₂ could be obtained by incorporating LiBH₄ with CaH₂, based on the formation of calcium hexaboride CaB₆ [21].

In view of the previous results mentioned above, a question arises as to whether other binary alkaline-earth metal hydrides than MgH₂ and CaH₂ can be used as the destabilizing additives for LiBH₄. Stimulated by this question, the dehydrogenation and rehydrogenation properties, as well as the destabilization mechanism involved for the LiBH₄/SrH₂ system have been investigated in this work. No catalysts were doped into the LiBH₄/SrH₂ system, which enables the investigation of the pure effect from SrH₂.

2. Experimental details

2.1. Sample preparation

Commercial LiBH₄ powder (95%, Alfa Aesar) was used as-received without further purification. SrH₂ powder was synthesized by reacting metallic Sr scraps (99%, Alfa Aesar) with hydrogen (99.999%). The 6LiBH₄ + SrH₂ mixture was ball-milled under 0.5 MPa hydrogen pressure at a rotation speed of 400 rpm for only 2 h by using a QM-1SP planetary mill. Stainless steel vials (250 mL in volume) and balls (10 mm in diameter) were used. The ball to sample weight ratio was 20:1. To avoid air-exposure, all sample handling was carried out in an Ar-filled glove box equipped with a purification system keeping the typical O₂/H₂O levels below 1 ppm.

2.2. Sample characterization

Dehydrogenation and rehydrogenation properties of the samples were examined based on the volumetric method by using a carefully calibrated Sieverts-type apparatus (Suzuki Shokan Co., Ltd., Japan). The temperature dependence of dehydrogenation was determined by heating the sample from ambient temperature to

* Corresponding author. Tel.: +86 555 2311891; fax: +86 555 2311570.

E-mail address: zhang03jp@yahoo.com.cn (Q.A. Zhang).

873 K at a heating rate of 2 K/min. Isothermal dehydrogenation was performed by quickly heating and then keeping the sample at a given temperature. The hydrogen back pressure for the above temperature ramp and isothermal dehydrogenation examinations was below 0.1 MPa. Pressure–composition (P–C) isotherms were measured at 693, 723 and 753 K to investigate the thermodynamic property of the $\text{LiBH}_4/\text{SrH}_2$ system in the dehydrogenation process. The rehydrogenation experiment was carried out at 723 K under an initial hydrogen pressure of 8.0 MPa.

To elucidate the phase components of the ball-milled, dehydrogenated and rehydrogenated $6\text{LiBH}_4 + \text{SrH}_2$ mixtures, X-ray diffraction (XRD) measurements were performed using a Rigaku D/Max 2500VL/PC diffractometer with $\text{Cu K}\alpha$ radiation at 50 kV and 150 mA. The XRD samples were loaded and sealed in a special holder that can keep the sample under argon atmosphere in the course of measurement.

3. Results and discussion

3.1. Dehydrogenation behavior

3.1.1. Thermal behavior upon dehydrogenation

For understanding the dehydrogenation stage of the $\text{LiBH}_4/\text{SrH}_2$ system, Fig. 1 gives the amount of hydrogen desorbed as a function of temperature for the as-milled $6\text{LiBH}_4 + \text{SrH}_2$ mixture at a heating rate of 2 K/min. For comparison, the hydrogen desorption curve of the pristine LiBH_4 sample ball-milled for 2 h was also measured. It is observed that dehydrogenation of the $\text{LiBH}_4/\text{SrH}_2$ system starts around 490 K, and the majority of hydrogen is released in the temperature range of 660–760 K. A dehydrogenation amount of 8.7 wt.% was totally achieved. In contrast, the pristine LiBH_4 released hydrogen sluggishly, and the amount of hydrogen desorbed up to 873 K is only 6.8 wt.%. This value is much lower than the theoretical one (13.8 wt.%). Evidently, the thermal stability of LiBH_4 can be remarkably reduced by using SrH_2 as a destabilizing additive.

It should be noted from Fig. 1 that dehydrogenation of the $\text{LiBH}_4/\text{SrH}_2$ system proceeds in a single step, i.e., through a direct reaction between LiBH_4 with SrH_2 . In comparison with the two-step dehydrogenation in the $\text{LiBH}_4/\text{MgH}_2$ system [25], such a feature enables the $\text{LiBH}_4/\text{SrH}_2$ system to release hydrogen prior to the decomposition of SrH_2 . That is, LiBH_4 is also effective in lowering the stability of SrH_2 , which is similar to the results observed in the $\text{LiBH}_4/\text{CaH}_2$ and $\text{LiBH}_4/\text{CaF}_2$ systems [7,21,26].

Fig. 2 presents the XRD patterns of the $6\text{LiBH}_4 + \text{SrH}_2$ samples after ball-milling and dehydrogenation at 723 K. It can be seen that the as-milled sample consists mainly of LiBH_4 and SrH_2 , indicating that no definite reaction occurred between the starting materials during milling. After dehydrogenation, as indicated in Fig. 2b, SrB_6 and LiH can be formed without the remaining LiBH_4 or SrH_2 . The XRD results suggest that the $\text{LiBH}_4/\text{SrH}_2$ system is dehydrogenated according to the following reaction:

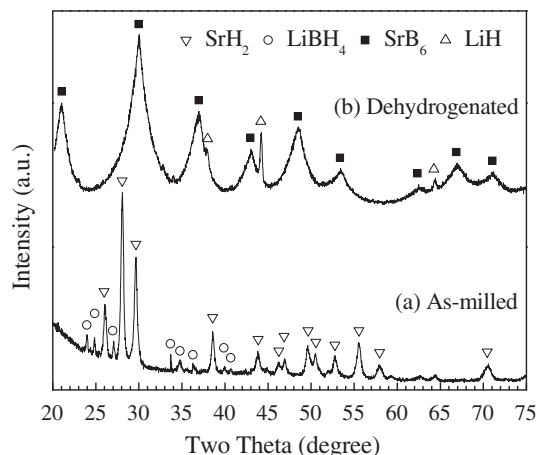
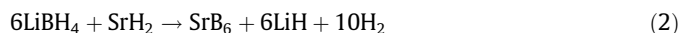


Fig. 2. XRD patterns of the $\text{LiBH}_4/\text{SrH}_2$ system: (a) as-milled and (b) dehydrogenated at 723 K.



The theoretical hydrogen amount desorbed from this reaction can be calculated to be 9.1 wt.%, which is consistent with the measured value of 8.7 wt.% (see Fig. 1).

3.1.2. Dehydrogenation thermodynamics

In order to evaluate the dehydrogenation thermodynamics of the $\text{LiBH}_4/\text{SrH}_2$ system, P–C isotherms (see Fig. 3) were measured at 693, 723 and 753 K, respectively. It can be seen that the dehydrogenation isotherms have a well-defined plateau region, and the equilibrium pressures vary from 0.49 MPa at 693 K to 0.94 MPa at 753 K. It is well known that the enthalpy change (ΔH) and entropy change (ΔS) for a dehydrogenation reaction can be calculated from the van't Hoff equation:

$$\ln P = [-\Delta H/(RT)] + \Delta S/R \quad (3)$$

where P is the equilibrium pressure at absolute temperature T , and R is the gas constant. Fig. 4 gives the van't Hoff plot of the $\text{LiBH}_4/\text{SrH}_2$ system by using the dehydrogenation equilibrium pressures at 4.0 wt.% (see Fig. 3). According to the equation shown in Fig. 4, the enthalpy and entropy changes for the dehydrogenation of the $\text{LiBH}_4/\text{SrH}_2$ system can be determined to be 48 kJ/mol H_2 and 82 J/(mol K) H_2 , respectively. The ΔS value here is rather different from the typical value of ~ 130 J/(mol K) H_2 for most metal hydrides. This difference can be mainly attributed to the higher entropy of LiBH_4

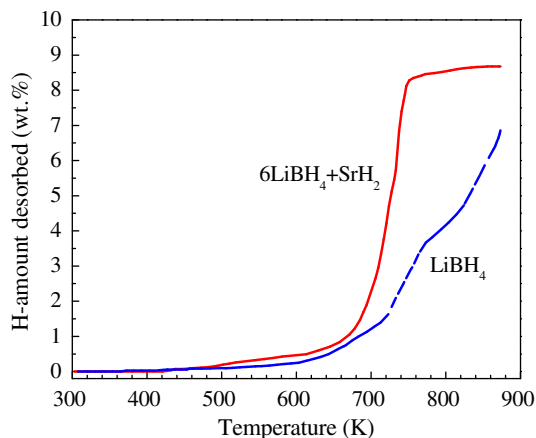


Fig. 1. Temperature dependence of dehydrogenation for the 2 h ball-milled $6\text{LiBH}_4 + \text{SrH}_2$ mixture and the pristine LiBH_4 at a heating rate of 2 K/min.

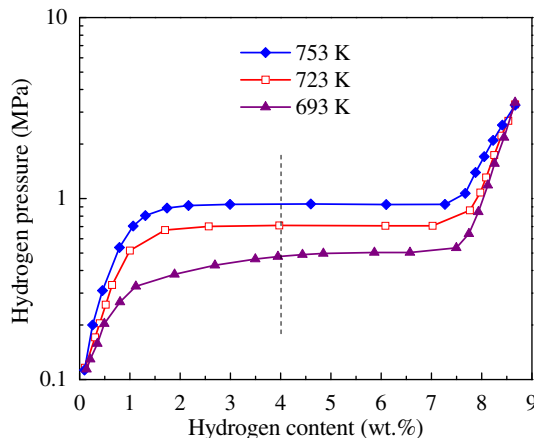


Fig. 3. Dehydrogenation P–C isotherms of the $\text{LiBH}_4/\text{SrH}_2$ system at different temperatures.

than LiH [27], and the lower ΔS value will result in a higher equilibrium dehydrogenation temperature under 0.1 MPa hydrogen pressure, $T(0.1 \text{ MPa})$. For the $\text{LiBH}_4/\text{SrH}_2$ system, extrapolation of the linear behavior shown in Fig. 4 gives the $T(0.1 \text{ MPa})$ value of 582 K.

Compared with the pristine LiBH_4 [4], the addition of SrH_2 lowers the enthalpy change of dehydrogenation by 26 kJ/mol H_2 . Hence, the stability of the $\text{LiBH}_4/\text{SrH}_2$ system decreases significantly. Note that the dehydrogenation enthalpy change (48 kJ/mol H_2) in the present case is lower than that for the $\text{LiBH}_4/\text{CaH}_2$ system (56.5 kJ/mol H_2 [21]), indicating that SrH_2 exhibits a somewhat stronger destabilization effect on LiBH_4 than its analog CaH_2 .

3.1.3. Dehydrogenation kinetics

Fig. 5 presents the isothermal dehydrogenation curves for the $\text{LiBH}_4/\text{SrH}_2$ system at 693, 723 and 753 K. It is clear that the $\text{LiBH}_4/\text{SrH}_2$ system desorbed hydrogen quickly at these temperatures. The amounts of hydrogen desorbed within 3600 s are 6.3, 8.0 and 8.5 wt.% at 693, 723 and 753 K, respectively. To further understand the dehydrogenation rate-limiting step of the $\text{LiBH}_4/\text{SrH}_2$ system, the isothermal curves were analyzed by the kinetic modeling, which can be generally expressed as the following equation:

$$g(\alpha) = \int d\alpha/f(\alpha) = kt \quad (4)$$

where α is the reacted fraction at time t , $g(\alpha)$ and $f(\alpha)$ are the functions representing the reaction mechanism of diffusion, nucleation and nuclei growth, or phase boundary, and so on, and k is the rate constant. In the present work, the reacted fraction was calculated by dividing the hydrogen amount desorbed at time t by the saturated dehydrogenation amount (8.7 wt.%). Then various mechanism functions, as described in the previous works [28,29], were tried to fit the experimental data shown in Fig. 5. As a result, the function $1 - (1 - \alpha)^{1/3}$ gives the best linearity over a broader range of α for each measurement, with the correlation coefficient of $R^2 > 0.998$. In Fig. 6, one can observe the linear relationships between $1 - (1 - \alpha)^{1/3}$ and t at 693, 723 and 753 K, respectively. This result suggests that the dehydrogenation process of the $\text{LiBH}_4/\text{SrH}_2$ system in the investigated temperature range is mainly rate-limited by the three-dimension phase boundary migration.

The rate constants at different temperatures were extracted from the slopes of the fitted straight lines shown in Fig. 6. As a result, the apparent activation energy E_a for dehydrogenation can be determined according to the Arrhenius equation:

$$k = k_0 \exp[-E_a/(RT)] \quad (5)$$

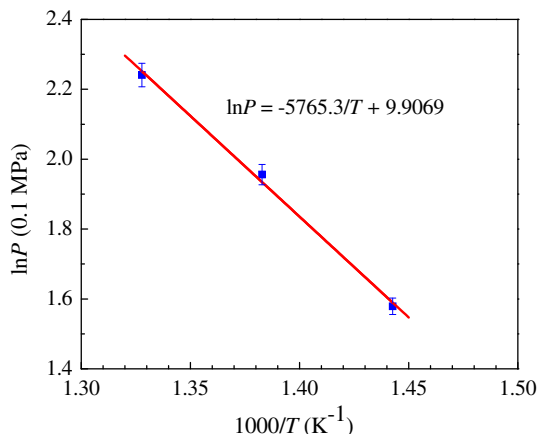


Fig. 4. Van't Hoff plot of the $\text{LiBH}_4/\text{SrH}_2$ system.

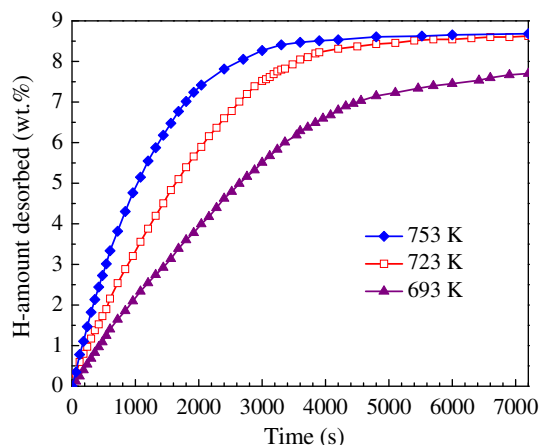


Fig. 5. Isothermal dehydrogenation curves of the $\text{LiBH}_4/\text{SrH}_2$ system at different temperatures.

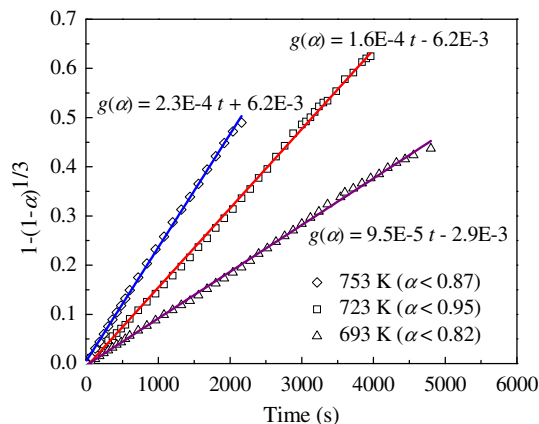
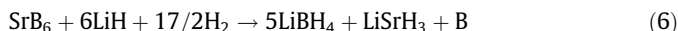


Fig. 6. Plots of $1 - (1 - \alpha)^{1/3}$ vs. t for the $\text{LiBH}_4/\text{SrH}_2$ system dehydrogenated at 693, 723 and 753 K, respectively.

where k_0 is the pre-exponential factor, R is the gas constant, and T is the absolute temperature. As shown in Fig. 7, a good linear relationship exists between $\ln k$ and $1/T$. From the slope ($-E_a/R$) of the straight line, E_a was calculated to be 64 kJ/mol for the $\text{LiBH}_4/\text{SrH}_2$ system. This value is much lower than that of the pristine LiBH_4 (111–156 kJ/mol [5,30,31]). The decrease in activation energy can be regarded as another reason contributing to the improved dehydrogenation property of the $\text{LiBH}_4/\text{SrH}_2$ system.

3.2. Rehydrogenation behavior

After dehydrogenation, the $\text{LiBH}_4/\text{SrH}_2$ system was subjected to rehydrogenation at 723 K under an initial hydrogen pressure of 8.0 MPa. Fig. 8a gives the isothermal rehydrogenation curve, indicating that 6.0 wt.% of hydrogen could be reabsorbed within 10 h. The XRD pattern for the rehydrogenated sample (shown in Fig. 8b) demonstrates that LiBH_4 was regenerated upon hydrogenation, even though the reverse reaction proceeded incompletely under the present experimental conditions. Moreover, LiSrH_3 is obviously observed in Fig. 8b. According to the XRD results, the rehydrogenation reaction for the $\text{LiBH}_4/\text{SrH}_2$ system can be deduced as:



In the recent work on the $\text{LiBH}_4/\text{CaF}_2$ system [26], it was considered that the rehydrogenation product CaB_6 could make the formation of $\text{LiB}_{12}\text{H}_{12}$ or LiBH_4 easier than that from B, owing to that CaB_6

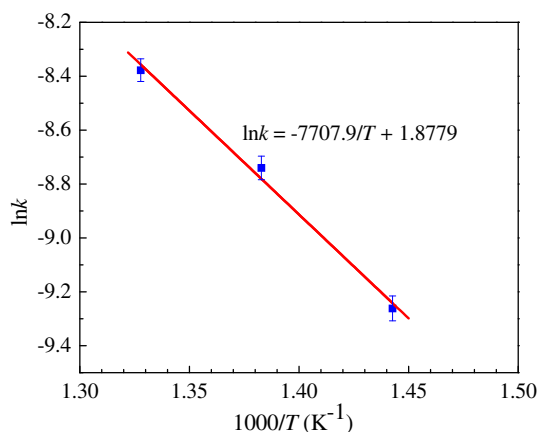


Fig. 7. Arrhenius plot for the dehydrogenation of the LiBH₄/SrH₂ system.

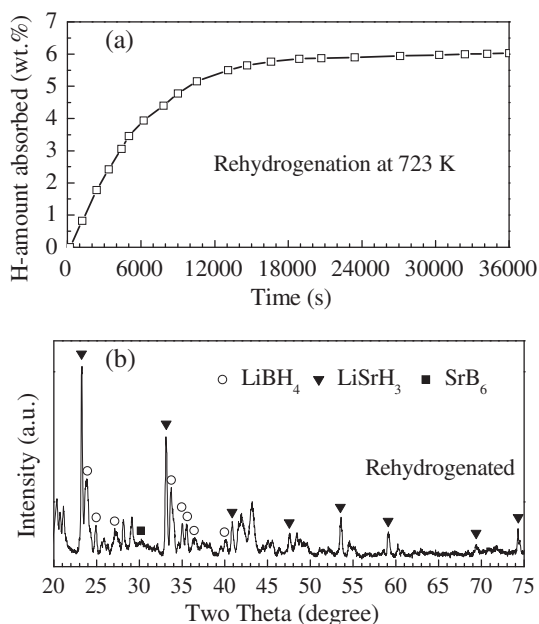


Fig. 8. (a) Isothermal rehydrogenation curve at 723 K and (b) XRD pattern of the rehydrogenated product for the LiBH₄/SrH₂ system.

has a structure close to the polyhedral structure in [B₁₂H₁₂]²⁻. Similar effect is believed to exist in the present case in view of the fact that SrB₆ has a CaB₆-type cubic structure [32].

4. Conclusions

In this paper, we report the dehydrogenation and rehydrogenation properties of a new reactive hydride system LiBH₄/SrH₂. It was found that the thermal stability of LiBH₄ can be remarkably reduced by the addition of SrH₂, *via* the reaction 6LiBH₄ + SrH₂ → SrB₆ + 6LiH + 10H₂ with a theoretical hydrogen capacity of

9.1 wt.%. The dehydrogenation enthalpy change for the LiBH₄/SrH₂ system is 48 kJ/mol H₂, which is reduced by 26 kJ/mol in comparison with pristine LiBH₄. The dehydrogenation process of the LiBH₄/SrH₂ system exhibits reduced activation energy of 64 kJ/mol. Moreover, the dehydrogenation process is rate-limited by a three-dimension phase boundary mechanism. Upon rehydrogenation at 723 K under an initial hydrogen pressure of 8.0 MPa, LiBH₄ can be regenerated with the formation of LiSrH₃.

Acknowledgements

This work was financially supported by the National Natural Science Foundation of China (No. 50901001), the Natural Science Foundation of Anhui Province (No. 1208085ME83) and the Scientific Research Foundation of Education Department of Anhui Province of China (No. KJ2010A044).

References

- [1] H.W. Li, Y. Yan, S. Orimo, A. Züttel, C.M. Jensen, *Energy* 4 (2011) 185.
- [2] C. Li, P. Peng, D.W. Zhou, L. Wan, *Int. J. Hydrogen Energy* 36 (2011) 14512.
- [3] Y. Bouhadda, S. Djellab, M. Bououdina, N. Fenineche, Y. Boudouma, *J. Alloys Compd.* 534 (2012) 20.
- [4] P. Mauron, F. Buchter, O. Friedrichs, A. Remhof, M. Biemann, C.N. Zwicky, A. Züttel, *J. Phys. Chem. B* 112 (2008) 906.
- [5] A. Züttel, S. Rentsch, P. Fischer, P. Wenger, P. Sudan, P. Mauron, C. Emmenegger, *J. Alloys Compd.* 356–357 (2003) 515.
- [6] J.J. Vajo, S.L. Skeith, F. Mertens, *J. Phys. Chem. B* 109 (2005) 3719.
- [7] F.E. Pinkerton, M.S. Meyer, *J. Alloys Compd.* 464 (2008) L1.
- [8] J. Mao, Z. Guo, X. Yu, H. Liu, *J. Alloys Compd.* 509 (2011) 5012.
- [9] Y. Jiang, B.H. Liu, *J. Alloys Compd.* 509 (2011) 9055.
- [10] Y. Zhang, Q. Tian, *Int. J. Hydrogen Energy* 36 (2011) 9733.
- [11] M. Meggouh, D.M. Grant, G.S. Walker, *J. Phys. Chem. C* 115 (2011) 22054.
- [12] D.M. Liu, Q.Q. Liu, T.Z. Si, Q.A. Zhang, F. Fang, D.L. Sun, L.Z. Ouyang, M. Zhu, *Chem. Commun.* 47 (2011) 5741.
- [13] F.C. Gennari, *Int. J. Hydrogen Energy* 36 (2011) 15231.
- [14] J.H. Shim, Y.S. Lee, J.Y. Suh, W. Cho, S.S. Han, Y.W. Cho, *J. Alloys Compd.* 510 (2012) L9.
- [15] X. Wu, X. Wang, G. Cao, S. Li, H. Ge, L. Chen, M. Yan, *J. Alloys Compd.* 517 (2012) 127.
- [16] Y. Zhou, Y. Liu, W. Wu, Y. Zhang, M. Gao, H. Pan, *J. Phys. Chem. C* 116 (2012) 1588.
- [17] J. Shao, X. Xiao, L. Chen, X. Fan, S. Li, H. Ge, Q. Wang, *J. Mater. Chem.* 22 (2012) 20764.
- [18] C. Luo, H. Wang, T. Sun, M. Zhu, *Int. J. Hydrogen Energy* 37 (2012) 13446.
- [19] S. Deng, X. Xiao, L. Han, Y. Li, S. Li, H. Ge, Q. Wang, L. Chen, *Int. J. Hydrogen Energy* 37 (2012) 6733.
- [20] J. Chen, Y. Zhang, Z. Xiong, G. Wu, H. Chu, T. He, P. Chen, *Int. J. Hydrogen Energy* 37 (2012) 12425.
- [21] J.H. Lim, J.H. Shim, Y.S. Lee, Y.W. Cho, *J. Lee, Scripta Mater.* 59 (2008) 1251.
- [22] Y. Zhou, Y. Liu, Y. Zhang, M. Gao, H. Pan, *Dalton Trans.* 41 (2012) 10980.
- [23] K. Jiang, X. Xiao, L. Chen, L. Han, S. Li, H. Ge, Q. Wang, *J. Alloys Compd.* 539 (2012) 103.
- [24] D. Liu, J. Yang, J. Ni, A. Drews, *J. Alloys Compd.* 514 (2012) 103.
- [25] U. Bösenberg, S. Doppiu, L. Mosegaard, G. Barkhordarian, N. Eigen, A. Borgschulte, T.R. Jensen, Y. Cerenius, O. Guttleisch, T. Klassen, M. Dornheim, R. Bormann, *Acta Mater.* 55 (2007) 3951.
- [26] P.P. Yuan, B.H. Liu, B.J. Zhang, Z.P. Li, *J. Phys. Chem. C* 115 (2011) 7067.
- [27] G. Walker, in: G. Walker (Ed.), *Solid-State Hydrogen Storage: Materials and Chemistry*, Woodhead Publishing Limited, Cambridge, 2008.
- [28] Y. Zhang, Q.F. Tian, J. Zhang, S.S. Liu, L.X. Sun, *J. Phys. Chem. C* 113 (2009) 18424.
- [29] Y. Li, G. Zhou, F. Fang, X. Yu, Q. Zhang, L. Ouyang, M. Zhu, D. Sun, *Acta Mater.* 59 (2011) 1829.
- [30] A.F. Gross, J.J. Vajo, S.L. Van Atta, G.L. Olson, *J. Phys. Chem. C* 112 (2008) 5651.
- [31] S. Kato, M. Biemann, A. Borgschulte, V. Zakaznova-Herzog, A. Remhof, S. Orimo, A. Züttel, *Phys. Chem. Chem. Phys.* 12 (2010) 10950.
- [32] C.H. Chen, T. Aizawa, N. Lyi, A. Sato, S. Otani, *J. Alloys Compd.* 366 (2004) L6.